The Tensile Fatigue Behavior of a GFRP Composite with Rubber Particle Modified Epoxy Matrix

C.M. Manjunatha, A.C. Taylor, A.J. Kinloch and S. Sprenger

Journal of Reinforced Plastics and Composites 2010 29: 2170 originally published online 8 September 2009
DOI: 10.1177/0731684409344652

The Tensile Fatigue Behavior of a GFRP Composite with Rubber Particle Modified Epoxy Matrix

C. M. MANJUNATHA,* A. C. TAYLOR AND A. J. KINLOCH
Department of Mechanical Engineering, Imperial College London, London, UK

S. SPRENGER
Nanoresins AG, Geesthacht, Germany

ABSTRACT: A thermosetting epoxy polymer was modified by incorporating 9 wt% of a CTBN rubber microparticles. The stress-controlled CA tensile fatigue behavior at stress ratio, $R = 0.1$ for both the neat and the modified epoxy was investigated. The addition of rubber particles increased the epoxy fatigue life by a factor of about three to four times. The rubber particle cavitation and plastic deformation of the surrounding material was observed to contribute to the enhanced fatigue life of the epoxy polymer. Then, the neat and the rubber-modified epoxy resins were infused into a quasi-isotropic, lay-up E-glass fiber, non-crimp fabric in a RIFT set -up to fabricate GFRP composite panels. Further, the stress-controlled CA tensile fatigue tests at stress ratio, $R = 0.1$ were performed on both of these GFRP composites. Matrix cracking and stiffness degradation was continuously monitored during the fatigue tests. Similar to bulk epoxy fatigue behavior, the fatigue life of GFRP composites increased by a factor of about three times due to the presence of rubber particles in the epoxy matrix. The suppressed matrix cracking and the reduced crack propagation rates in the rubber-modified matrix contribute towards the enhanced fatigue life of GFRP composites employing a rubber-modified epoxy matrix.

KEY WORDS: GFRP composite, fatigue, rubber-modified epoxy, thermosetting epoxy matrices, toughening mechanisms.

INTRODUCTION

DUE TO THEIR high specific strength and stiffness, fiber-reinforced polymer (FRP) composites are widely used in ship hull, airframe, and wind-turbine structural applications. The components in such structures invariably experience various types of constant and variable amplitude fatigue loads in service. Thus, safe operation of the structure for the required technical lifetime demands that such composite materials, in addition to their good static mechanical properties, need to possess a relatively high fatigue durability and fracture toughness.

*Author to whom correspondence should be addressed. E-mail: manjucm@nal.res.in
Figures 1, 3, 4 and 6–10 appear in color online: http://jrp.sagepub.com

0731-6844/10/14 2170–14 $10.00/0 DOI: 10.1177/0731684409344652

The majority of engineering composite materials in service consist of continuous fibers of glass, or carbon, reinforcing an epoxy polymeric matrix. The epoxy, when polymerized, is an amorphous and a highly cross-linked material. This microstructure of the epoxy polymer results in many useful properties such as high modulus and failure strength, low creep, etc., but also leads to an undesirable property in that it is relatively brittle and has a relatively poor resistance to crack initiation and growth. These adverse fracture properties may obviously also affect the overall fatigue and fracture performance of the FRP composites.

One of the ways to enhance the mechanical properties of FRP composites is to improve the properties of the epoxy matrix by incorporating second-phase modifiers in the resin. Various types of micro- and nano-sized particles, such as rubber and silica, have been employed to enhance the fracture toughness and fatigue behavior of epoxy polymers and FRP composites [1–12]. More recently, fibrous fillers such as carbon nanofibers [13], nanotubes [14], and layered fillers such as silicate-clay [15], have also been used to try to improve the composite properties.

The effect of rubber particles on the mechanical properties of epoxy polymers and FRP composites has been extensively investigated. The phase-separation of well-dispersed rubber microparticles, in the range of 5–20 vol.%, in the epoxy has been shown to significantly improve the fracture toughness of both bulk epoxy polymers and FRP composites using such modified polymers as the matrix [1,2,4,9,11]. For example, increases in the toughness, as high as a factor of about 10–15 times, have been reported for thermosetting epoxy polymers, without impairing the other desirable engineering properties [16]. Further, FRP composites based upon rubber particle reinforced matrices, have also shown a significant improvement in their values of interlaminar fracture toughness [9,11,17].

Although several fatigue crack propagation studies have been undertaken on rubber-modified bulk epoxy polymers [5–8], studies on the cyclic fatigue behavior of FRP composites based upon rubber-modified epoxy matrices are limited. Hence, the main aim of this investigation was to study the stress-controlled high-cycle fatigue behavior of a glass fiber-reinforced polymer (GFRP) composite based upon a rubber-modified epoxy matrix.

EXPERIMENTAL

Materials

The materials were based upon a single-component hot-cured epoxy formulation. The epoxy resin was a standard diglycidyl ether of bis-phenol A (DGEBA) with an epoxide equivalent weight (EEW) of 185 g/eq, 'LY556' supplied by Huntsman, Duxford UK. The reactive liquid rubber, which gives rise to the micrometer-sized spherical rubber particles upon curing of the formulation, was a carboxyl-terminated butadiene-acrylonitrile (CTBN) rubber. It was supplied by Emerald Materials, Akron, USA, and was 'Hycar CTBN 1300 × 8' with a number-average molecular weight of 3550 g/mol and an acrylonitrile content of 18 wt%. This was pre-reacted with the DGEBA resin to give a 40 wt% CTBN-epoxy adduct, 'Albipox 1000' (EEW =330 g/eq), from Nanoresins, Geesthacht, Germany. The curing agent was an accelerated methylhexahydrophthalic acid anhydride, 'Albidur HE 600' (AEW =170 g/eq), also supplied by Nanoresins. The E-glass fiber cloth was a non-crimp-fabric (NCF) roll with two layers of fiber arranged in a $\pm 45^{\circ}$ pattern with an areal weight of 450 g/m^2 from SP Systems, Newport, UK.

Processing

The required quantity of the neat DGEBA epoxy resin was weighed and degassed at 50°C. The calculated quantity of CTBN-epoxy adduct, to give the required level of 9 wt% added CTBN rubber in the final resin mixture, was also weighed and degassed. They were then mixed together and the value of the EEW of the blend was measured via titration. The stoichiometric amount of curing agent was added to the mixture. Typically, to prepare a 500 mL (555.3 g) rubber-modified resin mixture, 118 mL (127.5 g) of Albipox, 161 mL (189.3 g) of LY556, and 221 mL (238.6 g) of HE600 was used. The entire resin mixture was then stirred and degassed once again at 50°C and −1 atm. for about an hour. The neat and rubber-modified resin mixtures thus prepared were then used to manufacture both bulk epoxy polymer sheets and the GFRP composite panels.

To manufacture the bulk epoxy sheets, the resin mixture was poured into a release-coated steel mold. The filled mold was then placed in a circulating air oven and the temperature was ramped to 100°C at 1°C/min, cured for 2 h, again ramped to 150°C at 1°C/min and then post-cured for 10 h. The resulting neat and rubber-modified bulk, epoxy sheets were about $200 \times 200 \times 5\,mm^3$ in size.

The GFRP composite panels with neat and rubber-modified epoxy matrices were manufactured by the resin infusion using the flexible tooling (RIFT) technique [18]. Glass fiber NCF cloth pieces, about $330\,mm^2$, were cut and laid up in a quasi-isotropic sequence $[(+45/-45/0/90)_s]_2$ with a fluid distribution mesh. The resin mixture was infused into the glass-cloth lay-up at 50°C and −1 atm. Once the infusion was complete, the temperature was raised at 1°C/min to 100°C and the composite laminate was cured for 2 h. The temperature was raised again at 1°C/min to 150°C and finally post-cured for 10 h. The vacuum was maintained throughout the curing cycle. The resulting GFRP composite laminates (with neat and rubber-modified epoxy matrices) were about 2.5–2.8 mm thick and had a fiber volume fraction of about 57%.

Bulk Epoxy Microstructure

The atomic force microscope (AFM), as explained in [19], was used to observe the microstructure of the bulk epoxy polymer. A smooth surface was first prepared by cutting a sample, using a microtome, at room temperature. The surface scans were then performed employing a tapping mode, using a silicon probe. The AFM phase image of the bulk epoxy polymer containing 9 wt% CTBN rubber particles is shown in Figure 1. It was observed that the rubber particles were evenly distributed in the epoxy polymer and had an average size of about 0.5–1 μm. The average interparticle distance measured was about 2.45 μm. Finally, the glass transition temperatures, T_g, values were obtained using dynamic mechanical thermal analysis at a frequency of 1 Hz and were 153°C and 149°C for the neat and rubber-modified epoxies, respectively. These values are not considerably dissimilar, and reveal that virtually all the rubber is present in the cured rubber-modified epoxy as a dispersed second phase; and the AFM micrographs indeed confirm that it is present as a quite well-dispersed particulate phase.

Tensile Properties

The tensile properties of the bulk epoxies and GFRP composites were determined according to ASTM D638 [20] and ASTM D3039M [21] test standard

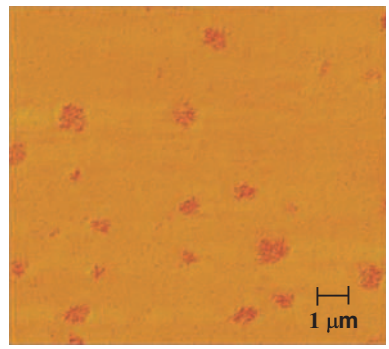

Figure 1. *The tapping mode AFM phase image of the 9 wt% rubber-modified bulk epoxy polymer.*

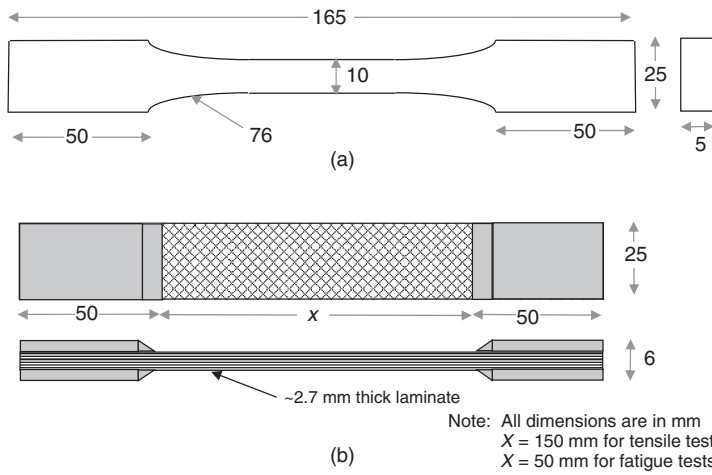

Figure 2. *Schematic diagrams showing the dimensions of the tensile and fatigue test specimens: (a) bulk epoxy polymer test specimen, (b) GFRP composite test specimen.*

specifications, respectively. Schematic diagrams showing the dimensions of tensile test specimen are shown in Figure 2. GFRP composite test specimens were end-tabbed, using GFRP composites (about 1.5 mm in thickness) to prevent damage to the specimen due to the grips during testing. All the tensile tests were performed using a 100 kN computer controlled screw-driven test machine, with a constant crosshead speed of 1 mm/min. An extensometer, with a 25 mm gauge length, was used to measure the displacement of the specimens. Five replicate tests were conducted for each material and the average tensile properties determined for all the materials are shown in Table 1.

As observed in an earlier investigation [22], the addition of the rubber particulate phase decreases the ultimate tensile strength (UTS) and modulus (E) of both the bulk epoxy and GFRP composite. Indeed, the UTS was decreased by about 11.2% and 5.2% for the bulk epoxy polymer and the GFRP composite, respectively. Similarly, the tensile modulus was observed to reduce by about 19.5 and 12.7% for the epoxy polymer and GFRP, respectively. Thus, as might be expected, the percentage reduction of the tensile properties induced by the presence of the rubber phase was observed to be relatively higher for the bulk epoxy polymer compared to the GFRP composite.

Table 1. Tensile properties of the bulk epoxy and GFRP composite.

Material	Condition	Tensile properties	
		UTS (MPa)	Modulus, *E* (GPa)
Bulk epoxy polymer	Neat epoxy	73.3 ± 1.4	2.62 ± 0.05
	Modified epoxy	65.1 ± 1.5	2.11 ± 0.03
GFRP composite	Neat matrix	364.8 ± 13.1	17.50 ± 0.60
	Modified matrix	345.9 ± 14.9	15.28 ± 0.42

Fatigue Testing

The fatigue test specimens were prepared from the bulk epoxy polymer sheets and GFRP composite panels. Schematic diagrams showing the dimensions of the fatigue test specimens are shown in Figure 2. The sharp edges of the bulk epoxy test specimens were smoothed with emery paper, before testing, to avoid any stress concentration effects. All the fatigue tests were performed according to the ASTM D3479M-96 test standard specifications [23], using a 25 kN computer-controlled servo-hydraulic test machine. The following fatigue parameters were employed for the tests: stress ratio, $R = 0.1$, sinusoidal waveform and frequency, $\nu = 1$–3 Hz. It should be noted that it has been shown that higher test frequencies may induce thermal effects, and lead to reduced fatigue lives in composites [24–26]. Therefore, the test frequency was kept below 3 Hz in the present studies.

The load vs. displacement data were obtained at specified regular intervals during the cyclic fatigue test, so that the stiffness of the specimen could be ascertained. About 100 pairs of load and displacement data were collected from the rising part of a fatigue cycle, and the stiffness was calculated by a linear regression analysis of the data. However, it was decided to use only about 50 data points in the central portion of the load vs. displacement data to perform the regression analysis in order to eliminate any possible non-linear effects introduced by the upper and lower end-points of the data sets. For the purpose of comparison, the normalized stiffness of the specimen was defined as the ratio of the initial stiffness (i.e., as obtained in the first cycle) to the measured stiffness at any given load cycle for the same test specimen.

The fracture surfaces from the fatigue tests of the bulk epoxy specimens were examined using a scanning electron microscope (SEM). The fracture surfaces were first sputter coated with a thin layer of gold, to prevent charging. Conventional secondary electron imaging conditions, with an accelerating voltage of 15 kV, were employed.

Measurement of Crack Density

Due to the translucent nature of the GFRP composite, the development of fatigue damage (i.e., matrix cracks and delaminations) was readily visible in the gauge section of the specimen during testing by using an illuminated light background. A detailed investigation of matrix cracking was performed during one of the fatigue tests (at a value of $\sigma_{max} = 150$ MPa) for both the GFRP composites manufactured with the neat and the rubber-modified matrix. An area, about $25 \times 25\,mm^2$, was marked at the center of the gauge section of the test specimen while the specimen was mounted in the test machine and a given number of fatigue cycles were applied. Then, the test was stopped, the specimen

was dismounted and the matrix cracks in the marked area were photographed, using a background projection of transmitted light. The specimen was then remounted and the test continued. This procedure was continued until the specimen failed.

A typical sequence of the photographic images obtained for the GFRP composite with a neat epoxy matrix is shown in Figure 3. The virgin sample with no matrix cracks is on the far left. The polyester binding yarns in both 0° and ±45° directions can be easily recognized (as faint, thick lines) but the E-glass fibers are not visible. With an increasing number of fatigue cycles, cracks were observed to develop in the +45°, −45°, and 90° directions, and become visible as dark lines in the respective directions. The higher the number of fatigue cycles, the greater the number of matrix cracks that developed. It is noteworthy that similar observation of such a sequence of matrix cracking in GFRP composites under cyclic fatigue testing has been reported earlier [27].

Although cracks in the 90° ply were observed in some images, they could not be consistently observed, due to the greater distance of this ply from the surface, and also due to the reduced transparency caused by the addition of the rubber phase. Gagel et al [27] observed that the stiffness of the composite in the first two stages of fatigue life correlated strongly with the density of the ±45° cracks, and only relatively weakly with the 90° ply cracks. Hence, only the ±45° cracks were considered for a detailed analysis in the present investigation. For the purpose of analysis, the crack density (CD), defined as the number of cracks per unit length, was determined by counting the visible ±45° cracks on an arbitrarily chosen line, which was drawn on such images as in Figure 3. Six repeat measurements were made on each of the photographic images, and the average value of the CD was obtained. It may be noted that there is always an uncertainty in the accuracy of such measurements, since the depth of focus can influence the CD measurements using the transmitted light photographic method. Hence, the CD measurements reported in the present study are used only for comparative purposes.

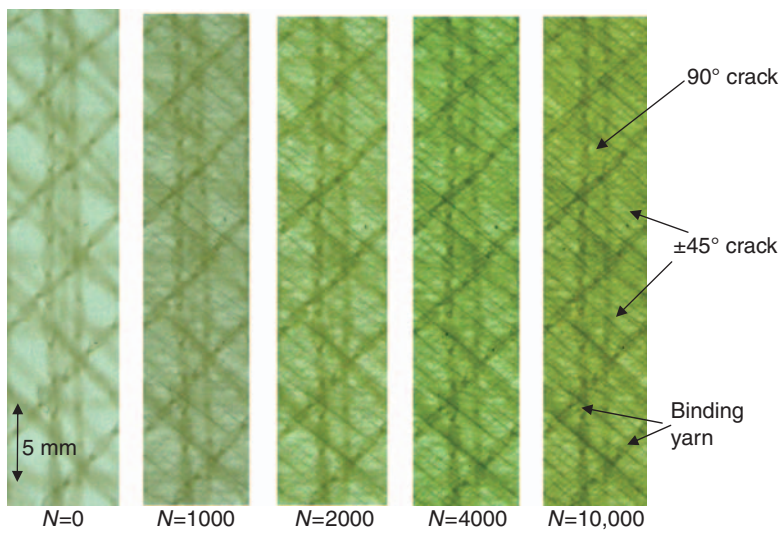

Figure 3. *The transmitted light photographic images of the GFRP composite with a neat matrix showing the sequence of matrix crack development with increasing number of cycles (N) under fatigue loading.*

RESULTS AND DISCUSSION

Fatigue Behavior of Bulk Epoxy Polymer

The constant-amplitude, tension-tension, cyclic-fatigue test results obtained for the neat and rubber particle modified bulk epoxy polymers at a stress ratio, $R = 0.1$, are shown in Figure 4. Here the vertical axis represents the maximum cyclic stress applied in the fatigue cycle and the horizontal axis represents the number of cycles to failure, i.e., typical 'S-N' curves. It may be clearly seen that, for a given maximum cyclic stress, the fatigue life of the 9 wt% rubber-modified epoxy polymer is higher than that of the neat epoxy, by about three to four times, and that this fatigue life enhancement appears over the entire range of the stress level investigated.

The experimental S-N data shown in Figure 4 was fit to Basquin's law [28]:

$$\sigma_{max} = \sigma'_f (N_f)^b \tag{1}$$

where σ'_f is the fatigue strength coefficient (FSC) and b is the fatigue strength exponent (FSE). The values of the parameters FSC and FSE, determined for both the neat and rubber-modified bulk epoxy polymers, are shown in Table 2. It can be seen that the presence of the rubber increases the value of the FSC by about 35%, whilst that of the FSE was observed to decrease by about 16%. It is of interest to note that Zhou, et al. [13]

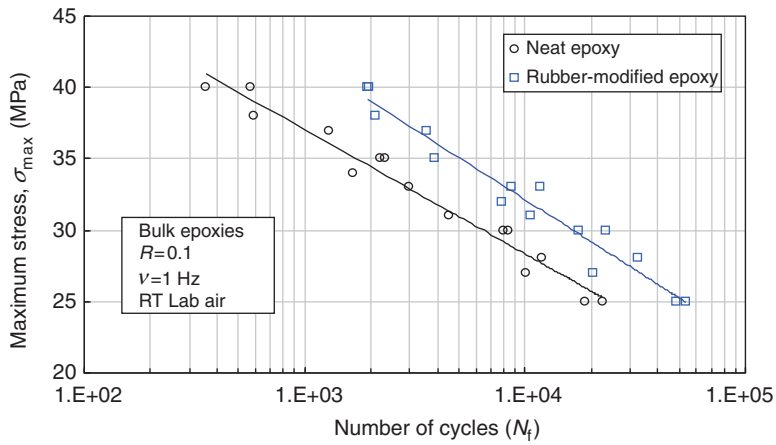

Figure 4. *The stress vs. lifetime (S-N) curves of the neat and 9 wt% rubber-modified bulk epoxy polymers.*

Table 2. Fatigue properties of the bulk epoxy polymers and the GFRP composites.

		Fatigue properties	
Material	**Condition**	**FSC (MPa)**	**FSE**
Bulk epoxy polymer	Neat resin	83.25	−0.1205
	Modified resin	108.52	−0.1406
GFRP composite	Neat matrix	462.48	−0.1121
	Modified matrix	531.00	−0.1133

have also observed quite similar trends in the variation of the fatigue properties for an epoxy polymer modified with carbon nanofibers.

It was observed that for both types of epoxy polymer that, in general, the fatigue crack initiated from the surface and propagated inside the test specimen in the form of a semi-elliptical, i.e., thumbnail, shaped crack. In accordance with general observations in polymers [29], a smooth, mirror-like region was exhibited by this initial fatigue crack growth region, which was followed by a radially lined, relatively rough, fast-fracture region.

The fatigue crack growth region of the bulk epoxy polymers was further examined, and SEM images of the fatigue fracture surfaces of both the neat and rubber particle modified epoxy polymers are shown in Figure 5. It can be seen in Figure 5(a) that the neat epoxy polymer has a relatively smooth fracture surface and is devoid of any indications of large-scale plastic deformation. However, the rubber-modified epoxy polymer (Figure 5(b)) exhibits a relatively rough fracture surface with clear indications of cavitated rubber microparticles and accompanying plastic deformation of the surrounding epoxy material. Indeed, similar fractographic features have been reported in a rubber-modified epoxy under fatigue loading [5].

The toughening mechanisms in rubber-modified epoxy polymers have been extensively investigated [2–8]. Essentially, the cavitation of the rubber particles leads to enhanced shear deformation of the epoxy polymer. This energy-dissipating mechanism has been shown to reduce the crack propagation rates significantly in a rubber-modified epoxy by up to an order of magnitude [5], hence resulting in an enhanced fatigue life compared with the neat epoxy polymer.

Fatigue Behavior of GFRP Composite

The stress controlled, constant-amplitude tensile fatigue test results at a stress ratio, $R = 0.1$, obtained for the GFRP composites with neat and rubber-modified epoxy matrices are shown in Figure 6. It may be seen that, over the entire range of stress level investigated, the rubber-modified epoxy matrix enhances the fatigue life of the GFRP composite by a factor of about three times, compared with employing the neat epoxy as the matrix material. It is noteworthy that Higashino et al. [10] have previously observed a similar significant improvement in fatigue life of carbon-fiber composites based upon a rubber-modified matrix.

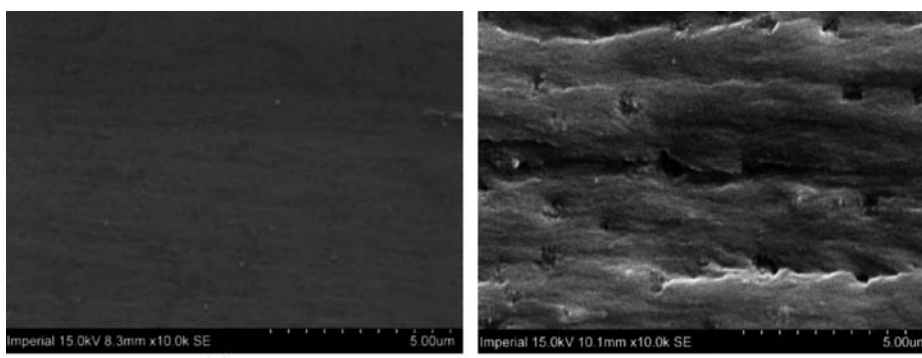

Figure 5. *The SEM of the fatigue fracture surfaces of bulk epoxy polymers (crack growth direction is from left to right): (a) neat epoxy, $\sigma_{max} = 37$ MPa, (b) rubber-modified epoxy, $\sigma_{max} = 37$ MPa.*

The experimental data of the 'S-N' curves of the GFRP composites shown in Figure 6 were fit to Equation (1) and the fatigue parameters from Basquin's law [28] (i.e., FSC and FSE) were determined and are shown in Table 2. Once again, as observed for bulk epoxy polymer, the FSC increased, by about 13%, due to addition of rubber particles in the epoxy matrix of GFRP. It may also be noted that the percentage increase in FSC of GFRP was relatively less compared to that observed in bulk epoxy. However, unlike the bulk epoxy polymer, the value of the FSE for the GFRP composite based upon the rubber-modified epoxy matrix remained very similar to that of GFRP based upon the neat epoxy matrix.

In all the fatigue tests, the stiffness of the specimen was observed to reduce with fatigue cycles. The normalized stiffness reduction with load cycles, evaluated for the fatigue test at $\sigma_{max} = 150$ MPa for the GFRP composites with neat and rubber-modified epoxy matrix is shown in Figure 7. In general, both GFRP composites exhibit a typical stiffness reduction

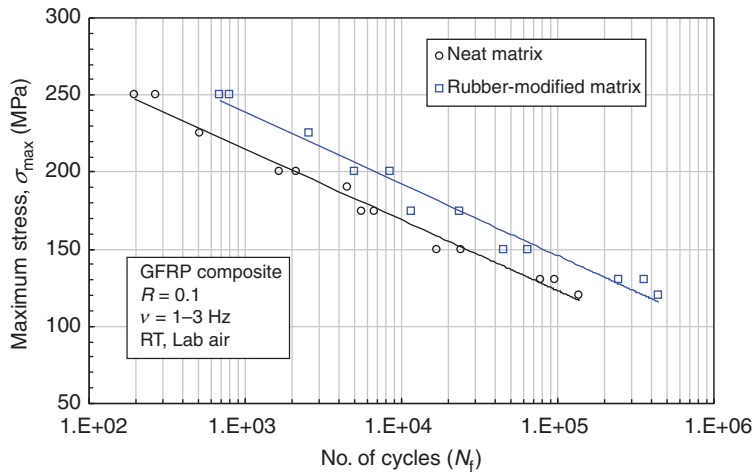

Figure 6. *The stress vs. life (S-N) curve of GFRP composites with neat and 9 wt% rubber-modified epoxy matrices.*

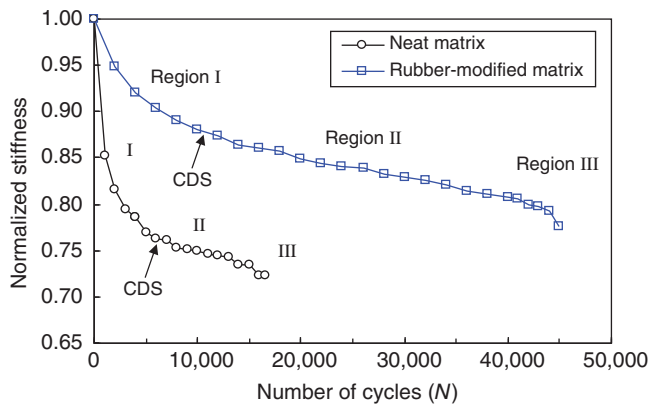

Figure 7. *The normalized stiffness variation during fatigue determined in GFRP composite with neat and rubber-modified epoxy matrices.* $\sigma_{max} = 150$ *MPa,* $R = 0.1$.

trend as observed in FRP composites [27,30–35]. The three regions of the stiffness reduction curve are clearly identifiable. It may be noted that the stiffness reduction in regions I and II was quite steep and significant in neat matrix GFRP composite when compared to GFRP with rubber-modified epoxy matrix.

The typical transmitted light photographic images obtained after subjecting the test specimens to fatigue loading for 10^3 cycles in GFRP composites with neat and rubber-modified epoxy matrix are shown in Figure 8. Both of the composites were observed to contain matrix cracks (visible as dark lines) in $\pm 45^\circ$ plies, evenly distributed over the entire area of the image. It may be clearly noted that for the same number of applied load cycles, the neat matrix GFRP composite appears to be more densely cracked than modified matrix GFRP.

The average CD of $\pm 45^\circ$ cracks, determined as a function of the fatigue cycles is shown in Figure 9. In both composites, the CD increased with load cycles and appears to saturate.

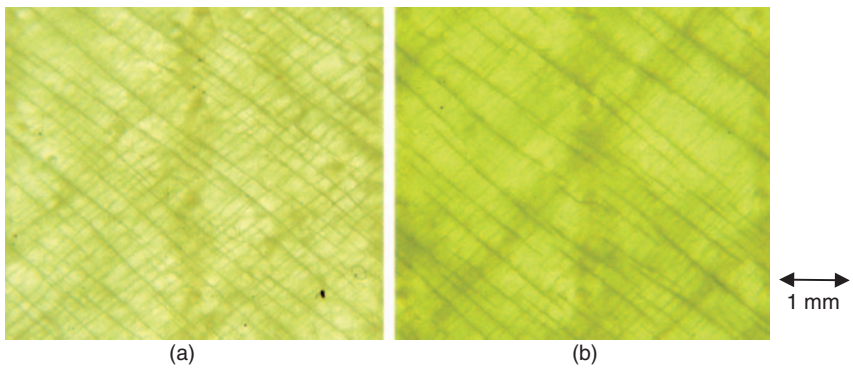

Figure 8. *The transmitted light photographic images showing the matrix cracking pattern in GFRP composites under fatigue loading. $\sigma_{max} = 150$ MPa, $N = 10{,}000$ cycles: (a) GFRP – Neat matrix, (b) GFRP – Rubber-modified matrix.*

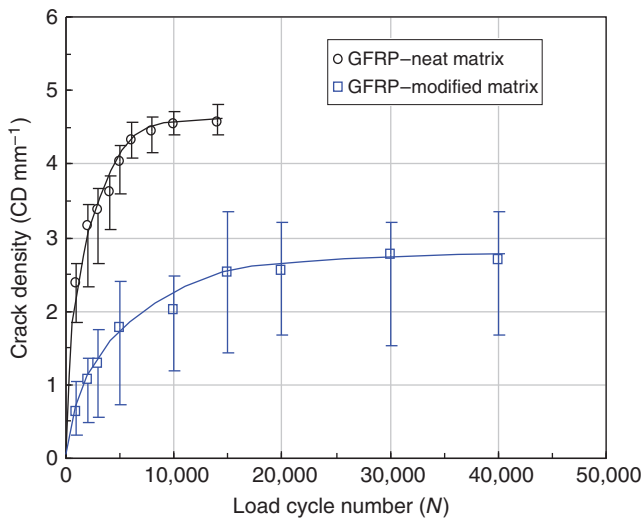

Figure 9. *The variation of $\pm 45^\circ$ crack density with fatigue cycles in GFRP composites based upon a neat or a rubber-modified matrix.*

The saturation level of CD was higher and about 4.5/mm in neat matrix GFRP whereas it was about 2.6/mm in modified matrix GFRP. It has been observed that such matrix crack saturation occurs in FRP composites [31,32] and this saturation level is independent of applied stress [37]. This saturation level of the progressive formation of matrix cracks, also termed as the characteristic damage state (CDS) [30,32] is reached much faster, in about 6000 load cycles, in neat matrix GFRP. The CDS appears to be delayed and occurs at about 15,000 cycles in GFRP with rubber-modified matrix. It is clear from Figure 9 that, for a given load cycle, GFRP with neat matrix is cracked considerably more than the GFRP with rubber-modified matrix, over the entire fatigue life of the composite.

The initiation and growth of interlaminar delaminations, particularly from the free edges of the test specimens, were observed with continued fatigue cycling. The typical photographic images showing the delamiantions at the free edges of GFRP composite with neat matrix is shown in Figure 10. Such free edge delaminations have been observed in composites, earlier [36]. The visible delamination initiation was observed at about 6000 and 15,000 cycles in neat and modified matrix GFRP composites respectively. It may be noted that the CDS was also observed to be reached at almost the same time (number of load cycles). The further growth of such delamination to critical size, led to final fatigue failure.

Based on the results obtained, the sequence of fatigue damage development leading to final failure, and hence defining the fatigue life in a QI lay-up GFRP composite, with neat and rubber particle modified epoxy matrix, can be briefly described as follows [30,32,37]. Initially, in both GFRP composites, matrix cracks develop (Figure 8) in the off-axis plies due to cyclic-fatigue loads. The density of these matrix cracks increase (Figure 9) and the cracks propagate with further continued application of load cycles, resulting in continuous decrease in the global stiffness of the composite (in region I of Figure 7). However, due to rubber particle toughened matrix, the matrix cracking is suppressed and crack density is lowered in GFRP with modified matrix (Figure 9). Also, from the epoxy fatigue studies, it is clear that fatigue life is enhanced due to reduced crack growth rates in modified epoxy (Figure 4 and Figure 5). It has been shown that fatigue crack growth rates in rubber-modified epoxy is over an order of magnitude lower than that in neat epoxy [5]. Thus, reduced cracking results in lowered degradation of the GFRP with modified matrix compared to neat matrix GFRP (Figure 7).

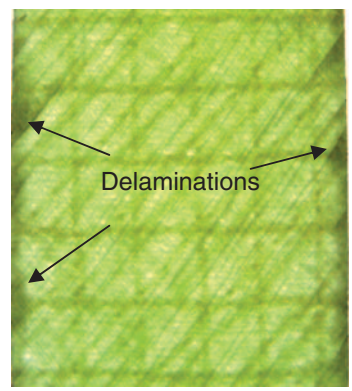

Figure 10. *The interlaminar delaminations observed at the free edges of the test specimen during fatigue testing of GFRP composite based upon a neat epoxy matrix.* $\sigma_{max} = 150$ *MPa and* $R = 0.1$.

The matrix cracking process continues until reaching CDS, from when the formation of secondary cracks in the epoxy matrix, perpendicular to primary cracks, leads to initiation of interlaminar delaminations (Figure 7 and Figure 10). Further growth of these damages lead to continued stiffness loss (in region II of Figure 7). Once again due probably to reduced delamination growth rates in rubber-modified epoxy, the stiffness reduction is much slower in modified matrix GFRP (Figure 7). It has been shown that simultaneously, dispersive and matrix crack-coupled [32] fiber breaking is an additional fatigue damage, which occurs during the entire fatigue life. We believe that such fiber breaks are probably delayed in modified matrix GFRP due to reduced crack growth rates in the presence of rubber particles. The accumulation and growth of all these damages leads to final fatigue failure of the composite but the modified matrix GFRP exhibits an improved fatigue life over that of neat matrix GFRP.

CONCLUSIONS

The following conclusions may be drawn based on the results obtained in this investigation.

(1) The fatigue life of 9 wt% rubber microparticle modified bulk epoxy is about three to four times higher than that of neat epoxy. The rubber particle cavitation and the plastic deformation of the surrounding material appear to contribute towards enhanced fatigue life in modified epoxy.
(2) The fatigue life of GFRP composite with 9 wt% rubber microparticle modified epoxy matrix is about three times higher than that of GFRP with neat matrix. The suppressed matrix cracking and reduced crack growth rate due to rubber cavitation and plastic deformation mechanisms appears to contribute to the observed enhancement of the fatigue life in GFRP with modified matrix.

ACKNOWLEDGMENTS

Dr C.M. Manjunatha wishes to thank the United Kingdom – India Education and Research Initiative (UKIERI) for the award of Research Fellowship. Thanks also go to Dr AR Upadhya, Director and Mr. DV Venkatasubramanyam, Head, STTD, National Aerospace Laboratories, Bangalore, India for permitting Dr CM Manjunatha to accept the Fellowship. The technical support staff members of the Department of Mechanical Engineering and the Composite Centre of Department of Aeronautics, Imperial College London are also thanked for their assistance in the experimental studies.

REFERENCES

1. Kinloch, A. J., Shaw, S. J., Tod, D. A. and Hunston, D. L. (1983). Deformation and Fracture Behavior of a Rubber Toughened Epoxy: Microstructure and Fracture Studies, *Polymer*, **24**(10): 1341–1354.
2. Kinloch, A. J. (2003). Toughening Epoxy Adhesives to Meet Today's Challenges, *MRS Bulletin*, **28**(6): 445–448.
3. Arias, M. L., Frontini, P. M. and Williams, R. J. J. (2003). Analysis of the Damage Zone Around the Crack Tip for Two Rubber-modified Epoxy Matrices Exhibiting Different Toughenability, *Polymer*, **44**(5): 1537–1546.

4. Pearson, R. A. and Yee, A. F. (1991). Influence of Particle Size and Particle Size Distribution on Toughening Mechanisms in Rubber Modified Epoxies, *Journal of Materials Science*, **26**(14): 3828–3844.
5. Azimi, H. R., Pearson, R. A. and Hertzberg, R. W. (1996). Fatigue of Rubber-modified Epoxies: Effect of Particle Size and Volume Fraction, *Journal of Materials Science*, **31**(14): 3777–3789.
6. Low, I. M. and Mai, Y. W. (1988). Micromechanisms of Crack Extension in Unmodified and Modified Epoxy Resins, *Composites Science and Technology*, **33**(3): 191–212.
7. Lowe, A., Kwon, A. H. and Mai, Y. W. (1996). Fatigue and Fracture Behaviour of Novel Rubber Modified Epoxy Resins, *Polymer*, **37**(4): 565–572.
8. Imanaka, M., Motohashi, S., Nishi, K., Nakamura, Y. and Kimoto, M. (2009). Crack-growth Behaviour of Epoxy Adhesives Modified with Liquid Rubber and Cross-linked Rubber Particles Under Mode I Loading, *International Journal of Adhesion and Adhesives*, **29**(1): 45–55.
9. Kinloch, A. J., Masania, K., Taylor, A. C., Sprenger, S. and Egan, D. (2008). The Fracture of Glass Fiber Reinforced Epoxy Composites Using Nanoparticle Modified Matrices, *Journal of Materials Science*, **43**(3): 1151–1154.
10. Higashino, M., Takemura, K. and Fujii, T. J. (1995). Strength and Damage Accumulation of Carbon Fabric Composites with a Cross-Linked NBR Modified Epoxy Under Static and Cyclic Loadings, *Composite Structures*, **32**(1–4): 357–366.
11. Caccavale, V., Wichmann, M. H. G., Quaresimin, M. and Schulte, K. (2007). Nanoparticle/Rubber Modified Epoxy Matrix Systems: Mechanical Performance in CFRPs, In: *AIAS XXXVI Convegno Nazionale*, Ischia, Napoli, 4–8 September.
12. Manjunatha, C. M., Taylor, A. C., Kinloch, A. J. and Sprenger, S. (2009). The Effect of Rubber Micro-Particles and Silica Nano-Particles on the Tensile Fatigue Behaviour of a Glass Fiber Epoxy Composite, *Journal of Materials Science*, **44**(1): 342–345.
13. Zhou, Y., Pervin, F., Jeelani, S. and Mallick, P. K. (2008). Improvement in Mechanical Properties of Carbon Fabric-Epoxy Composite Using Carbon Nanofibers, *Journal of Materials Processing Technology*, **198**(1–3): 445–453.
14. Gojny, F. H., Wichmann, M. H. G., Fiedler, B., Bauhofer, W. and Schulte, K. (2005). Influence of Nano-modification on the Mechanical and Electrical Properties of Conventional Fiber-reinforced Composites, *Composites Part A*, **36**: 1525–1535.
15. Zhou, Y., Rangari, V., Mahfuz, H., Jeelani, S. and Mallik, P. K. (2005). Experimental Study on Thermal and Mechanical Behaviour of Polypropylene, Talc/polypropylene and Polypropylene/Clay Nanocomposites, *Materials Science and Engineering A*, **402**(1–2): 109–117.
16. Kinloch, A. J., Mohammed, R. D., Taylor, A. C., Eger, C., Sprenger, S. and Egan, D. (2005). The Effect of Silica Nano Particles and Rubber Particles on the Toughness of Multiphase Thermosetting Epoxy Polymers, *Journal of Materials Science*, **40**(18): 5083–5086.
17. Kinloch, A. J., Mohammed, R. D., Taylor, A. C., Sprenger, S. and Egan, D. J. (2006). The Interlaminar Toughness of Carbon Fiber Reinforced Plastic Composites Using Hybrid Toughened Matrices, *Journal of materials Science*, **41**(15): 5043–5046.
18. Summerscales, J. and Searle, T. J. (2005). Low-Pressure (Vacuum Infusion) Techniques for Moulding Large Composite Structures, *Journal of Materials: Design and Application*, **219**: 45–58.
19. Johnsen, B. B., Kinloch, A. J., Mohammed, R. D., Taylor, A. C. and Sprenger, S. (2007). Toughening Mechanisms of Nanoparticle-modified Epoxy Polymers, *Polymer*, **48**(2): 530–541.
20. American Society for Testing and Materials (2003). *Standard Test Method for Tensile Properties of Plastics, ASTM D638-01, Annual Book of ASTM Standards*, Vol 8.02, American Society for Testing and Materials, PA.
21. American Society for Testing and Materials (2003). *Standard Test Method for Tensile Properties of Polymer Matrix Composite Materials, ASTM D3039, Annual Book of ASTM Standards*, Vol. 15.03, American Society for Testing and Materials, PA.
22. Garg, A. C. and Mai, Y. W. (1988). Failure Mechanisms in Toughened Epoxy Resins – A Review, *Composites Science and Technology*, **31**(3): 179–223.
23. American Society for Testing and Materials (2003). *Standard Test Method for Tension-Tension Fatigue of Polymer Matrix Composite Materials, ASTM D3479M-96, Annual Book of ASTM Standards*, Vol. 8.02, American Society for Testing and Materials, PA.
24. Mandell, J. F. and Meier, U. (1983). Effect of Stress Ratio, Frequency and Loading Time on the Tensile Fatigue of Glass-reinforced Epoxy, In: O'Brien, T. K. (ed.), *Long-term Behaviour of Composites, ASTM STP 813*, pp. 55–77, ASTM International, West Conshohocken, PA.
25. Staff, C. R. (1983). Effect of Load Frequency and Lay-Up on Fatigue Life of Composites, In: O'Brien, T. K. (ed.), *Long-term Behaviour of Composites, ASTM STP 813*, pp. 78–91, ASTM International, West Conshohocken, PA.
26. Sun, C. T. and Chan, W. S. (1979). Frequency Effect on the Fatigue Life of a Laminated Composite, In: Tsai, S. W. (ed.), *Composite Materials: Testing and Design (Fifth Conference), ASTM STP 674*, pp. 418–430, ASTM International, West Conshohocken, PA.
27. Gagel, A., Lange, D. and Schulte, K. (2006). On the Relation between Crack Densities, Stiffness Degradation, and Surface Temperature Distribution of Tensile Fatigue Loaded Glass-Fiber Non-Crimp-Fabric Reinforced Epoxy, *Composites Part A: Applied Science and Manufacturing*, **37**(2): 222–228.

28. Buch, A. (1988). *Fatigue Strength Calculation*, Transtech Publications, Switzerland.
29. Sauer, J. A. and Richardson, G. C. (1980). Fatigue of Polymers, *International Journal of Fracture*, **16**(6): 499–532.
30. Talreja, R. (1981). Fatigue of Composite Materials: Damage Mechanisms and Fatigue Life Diagrams, *Proceedings of Royal Society of London A*, **378**: 461–475.
31. Hahn, H. T. and Kim, R. Y. (1976). Fatigue Behaviour of Composite Laminates, *Journal of Composite Materials*, **10**: 156–180.
32. Case, S. W. and Reifsnider, K. L. (2003). Fatigue of Composite Materials, In: Milne, I., Ritchie, R. O. and Karihaloo, B. (eds), *Comprehensive Structural Integrity, Vol. 4: Cyclic Loading and Fatigue*, **1st edn**, Elsevier Science, Amsterdam.
33. Tate, J. S. and Kelkar, A. D. (2008). Stiffness Degradation Model for Biaxial Braided Composites under Fatigue Loading, *Composites Part B: Engineering*, **39**(3): 548–555.
34. Lee, J., Fu, K. E. and Yang, J. N. (1996). Prediction of Fatigue Damage and Life for Composite Laminates Under Service Loading Spectra, *Composites Science and Technology*, **56**(6): 635–648.
35. Reifsnider, K. L. and Jamison, R. (1982). Fracture of Fatigue-loaded Composite Laminate, *International Journal of Fatigue*, **4**(4): 187–192.
36. Case, S. W., Caliskan, A., Iyengar, N. and Reifsnider, K. L. (1996). Performance simulation of High-Temperature Polymericcomposite Materials using MRLife, In: *Proceedings of the ASME Aerospace Division—1996 ASME International Mechanical Engineering Congress and Exposition*, pp. 375–380.
37. Reifsnider, K. (1980). Fatigue Behaviour of Composite Materials, *International Journal of Fracture*, **16**(6): 563–583.